AJNR

Characteristics of Diffusional Kurtosis in Chronic Ischemia of Adult Moyamoya Disease: Comparing Diffusional Kurtosis and Diffusion Tensor Imaging

K. Kazumata, K.K. Tha, H. Narita, Y.M. Ito, H. Shichinohe, M. Ito, H. Uchino and T. Abumiya

Characteristics of Diffusional Kurtosis in Chronic Ischemia of Adult Moyamoya Disease: Comparing Diffusional Kurtosis and Diffusion Tensor Imaging

K. Kazumata, K.K. Tha, H. Narita, Y.M. Ito, H. Shichinohe, M. Ito, H. Uchino, and T. Abumiya

ABSTRACT

BACKGROUND AND PURPOSE: Detecting microstructural changes due to chronic ischemia potentially enables early identification of patients at risk of cognitive impairment. In this study, diffusional kurtosis imaging and diffusion tensor imaging were used to investigate whether the former provides additional information regarding microstructural changes in the gray and white matter of adult patients with Moyamoya disease.

MATERIALS AND METHODS: MR imaging (diffusional kurtosis imaging and DTI) was performed in 23 adult patients with Moyamoya disease and 23 age-matched controls. Three parameters were extracted from diffusional kurtosis imaging (mean kurtosis, axial kurtosis, and radial kurtosis), and 4, from DTI (fractional anisotropy, radial diffusivity, mean diffusivity, and axial diffusivity). Voxelwise analysis for these parameters was performed in the normal-appearing brain parenchyma. The association of these parameters with neuropsychological performance was also evaluated.

RESULTS: Voxelwise analysis revealed the greatest differences in fractional anisotropy, followed, in order, by radial diffusivity, mean diffusivity, and mean kurtosis. In patients, diffusional kurtosis imaging parameters were decreased in the dorsal deep white matter such as the corona radiata and superior longitudinal fasciculus ($P < .01$), including areas without DTI abnormality. Superior longitudinal fasciculus fiber-crossing areas showed weak correlations between diffusional kurtosis imaging and DTI parameters compared with tissues with a single-fiber direction (eg, the corpus callosum). Diffusional kurtosis imaging parameters were associated with general intelligence and frontal lobe performance.

CONCLUSIONS: Although DTI revealed extensive white matter changes, diffusional kurtosis imaging additionally demonstrated microstructural changes in ischemia-prone deep white matter with abundant fiber crossings. Thus, diffusional kurtosis imaging may be a useful adjunct for detecting subtle chronic ischemic injuries.

ABBREVIATIONS: AD = axial diffusivity; AK = axial kurtosis; CPT = continuous performance task; DKI = diffusional kurtosis imaging; FA = fractional anisotropy; IQ = intelligence quotient; MK = mean kurtosis; MD = mean diffusivity; MMD = Moyamoya disease; RD = radial diffusivity; RK = radial kurtosis; RST = Reading Span Test; SLF = superior longitudinal fasciculus; TMT = Trail-Making Test

Moyamoya disease (MMD) is characterized by compensatory development of enlarged and weak basal perforating arteries (Moyamoya vessels) due to bilateral occlusive changes in the internal carotid system.[1] In addition to cerebral ischemia and intracranial hemorrhage, patients with MMD demonstrate neurocognitive issues, such as executive dysfunction, attention deficits,

and working-memory disturbances.[2,3] Brain atrophy may explain cognitive impairment in the absence of infarction, but detection of these changes has been hampered by the limited sensitivity of conventional neuroimaging methods. Diffusion tensor imaging is useful for determining white matter integrity and providing parameters sensitive to changes in axons, myelin, and organelle structures.[4,5] Indeed, DTI analysis has revealed a widespread decline in white matter integrity in the normal-appearing brain with MMD.[3] Thus, DTI can detect

Table 1: Characteristics of the study participants

	Control	Moyamoya Disease	P Value
No. of subjects	23	23	–
Age (mean) (range) (yr)	39.0 + 8.1 (25–56)	40.9 + 9.5 (21–58)	.48
Sex (F/M) (No. of subjects)	13:10	17:6	.35
Risk factor (DM, HT, HL) (No. of subjects)	0	5	.049
Symptoms (No. of subjects)			
Asymptomatic	–	13	
TIA	–	10	

Note:—DM indicates diabetes mellitus; HT, hypertension; HL, hyperlipidemia.

early-stage ischemic injury, which potentially predicts future cognitive outcomes. However, DTI is constrained by technical insufficiencies: It is based on the assumption that water molecules diffuse freely and that diffusion can be characterized by a Gaussian distribution.[5]

In addition, the tensor model is based on the observation that in many tissues, water diffusion is anisotropic (ie, the diffusion is more liberal in some directions and more restricted in others). This anisotropic diffusion can be geometrically depicted as an ellipsoid, described by eigenvectors and eigenvalues. This model performs well in regions where fibers are aligned along a single axis. However, it fails in regions with several fiber populations aligned along intersecting axes because it cannot simultaneously map several diffusion maxima.[6] Furthermore, because hypoxic-ischemic injury induces neurodegeneration and regression of dendrite arborization in gray matter, the diffusion properties of gray matter may also reveal the early stages of ischemic injury.[7,8] Nevertheless, analyzing isotropic or near-isotropic tissue such as gray matter by DTI may not be valid because its major parameter, fractional anisotropy (FA), reflects structure only if it is spatially oriented.[6] A more recent method called diffusional kurtosis imaging (DKI) quantifies the deviation of water molecule diffusion from the Gaussian distribution without assuming any specific diffusion model.[6,9] Its parameters are thought to represent the complexity of tissue microstructure.[6] Previous studies have suggested that DKI is sufficiently sensitive to detect age-related alterations in white matter microstructure.[10,11] Furthermore, measurements of diffusion anisotropy by DKI can reveal sex-related and pathologic changes in gray matter.[12,13] Thus, using DKI to evaluate the diffusion properties of gray matter and white matter in patients with MMD may be useful for detecting subtle microstructural changes due to ischemia.

Diffusional kurtosis has been investigated to explore tissue reversibility in acute cerebral infarction.[14-16] However, there is a paucity of information regarding the microstructural properties measured by DKI in chronic ischemia in living humans. To expand on our prior DTI study, we investigated whether adults with MMD and no overt cerebral infarctions have altered diffusional kurtosis in the entire cerebrum. An exploratory voxel-based whole-brain analysis was performed to map regional DKI parameters and to compare DKI and DTI parameters. We also explored correlations of diffusion parameters with measures of neurocognitive impairment in an ROI analysis.

MATERIALS AND METHODS

Participants

This prospective study was approved by the Research Ethics Committee of Hokkaido University Hospital, and written informed consent was obtained from all participants. Participants in the present study are the same as those of our previous study analyzing the relationship between DTI parameters and neuropsychological test scores.[3] The selection period was 25 months (April 2012 through April 2014). Twenty-three patients (6 men and 17 women; 21–58 years of age; mean age, 40.9 ± 9.5 years) were enrolled. The control group also consisted of 23 subjects (10 men and 13 women; 25–56 years of age; mean age, 39.0 ± 8.1 years). A brief summary of patient characteristics is provided in Table 1.

Neuropsychological Assessment

Neuropsychological examinations consisted of the Wechsler Adult Intelligent Scale-III, Wisconsin Card Sorting Test, Trail-Making Test (TMT; parts A and B), continuous performance task (CPT), Stroop test, and Reading Span Test (RST). The details of neuropsychological examinations and the results are provided in the On-line Appendix.[3]

MR Image Acquisition

MR imaging was performed with a 3T scanner (Achieva TX; Philips Healthcare, Best, the Netherlands). 3D magnetization-prepared rapid acqustion of gradient echo T1-weighted imaging and axial single-shot spin-echo echo-planar DKI were acquired to evaluate subtle gray and white matter alterations, respectively. The scan parameters for DKI were as follows: TR = 5051 ms, TE = 85 ms, flip angle = 90°, FOV = 224 × 224 mm^2, matrix size = 128 × 128, b-values = 0, 1000, and 2000 s/mm^2, number of diffusion gradient directions = 32, section thickness = 3 mm, intersection gap = 0 mm, number of sections = 43, and NEX = 1. The 3D-MPRAGE imaging was performed with TR = 6.8 ms, TE = 3.1 ms, flip angle = 8 °, and TI = 1100 ms.

Image Processing

Registration between the echo-planar images with no diffusion weighting ($b=0$ s/mm^2) and the corresponding DKI data and correction for eddy current distortion were performed at the MR imaging operator console. The DKI data were processed by using Matlab R2012b (MathWorks, Natick, Massachusetts) and Diffusional Kurtosis Estimator (Version 2.5.1; http://nitrc.org/projects/dke).[17] Seven DKI and DTI parameters were extracted from the Diffusional Kurtosis Estimator: mean kurtosis (MK), radial kurtosis (RK), axial kurtosis (AK), FA, mean diffusivity (MD), radial diffusivity (RD), and axial diffusivity (AD). The DTI parameters (FA, MD, RD, and AD) were calculated from a portion of the DKI data by using a monoexponential model that assumes a Gaussian probability diffusion function by using data from b-values of 0 and 1000 s/mm^2.[17]

Following calculation of DKI and DTI parameters, the $b=0$ echo-planar images were warped to the standardized T2 template

of SPM8 (http://www.fil.ion.ucl.ac.uk/spm/software/spm12). This transformation matrix was applied to the DKI/DTI parameter map of each patient. The warped DKI/DTI maps were averaged and smoothed with a 6-mm full width at half maximum Gaussian kernel to form customized DKI/DTI templates. Native DKI/DTI maps of all patients and control subjects were then warped to the customized, respective DKI/DTI templates. Individual maps were then smoothed with a 6-mm full width at half-maximum Gaussian kernel. The warped and smoothed DKI/DTI maps were used for group comparisons between the controls and patients with MMD. To investigate the pathology underlying DKI parameters and the influence of fiber crossings on DTI parameters, we investigated the correlations of DKI and DTI parameters in white matter tracts consisting of either a single fiber direction or crossing fibers (ie, multiple directions).[18] The ROIs were placed on the genu of the corpus callosum (ie, a structure with a single fiber direction) and deep white matter tracts corresponding to the bilateral superior longitudinal fasciculus (SLF) (multiple fiber directions) by using the JHU white matter atlas available in FSL (http://fsl.fmrib.ox.ac.uk/fsl/fslwiki/).[19]

Data Analysis

Whole-brain diffusion parameters were compared voxel by voxel between the controls and patients with MMD by using SPM8, which implemented the general linear model. We used the 2-sample t test model, and age was considered a covariate. An explicit mask generated by averaging the normalized CSF space of all participants was applied. To explore group differences across both gray matter and white matter, we set statistical significance at $P <$ .01 without correction for family-wise error and clusters of 50 voxels or more. The number of voxels demonstrating a significant difference between the controls and patients with MMD was extracted. The Pearson product-moment correlation coefficient was calculated to investigate the correlation between the DKI and DTI parameters by using DKI/DTI values extracted from the ROI analysis.

We also investigated whether the significant changes in DKI/DTI parameters were associated with neuropsychological examination scores. A threshold T value of 2.42, corresponding to $P <$ .01 without correction for family-wise error, was applied to the T contrast map of DKI/DTI parameters obtained by comparing controls and patients, and binary mask images containing voxels above the threshold value were generated. The DKI/DTI parameter values included in the masks were extracted from DKI/DTI of the patients with MMD. The Pearson product-moment correlation coefficients were used for analyses involving the Wechsler Adult Intelligent Scale-III, TMT (parts A and B and the difference in score between TMT-A and TMT-B [B–A]). Patients were further subgrouped into 2, according to their performance scores, error numbers, and reaction time on the Wisconsin Card Sorting Test, Stroop test, CPT, and RST; and the DKI/DTI parameters were compared between these 2 subgroups by using t tests (Online Appendix). For all correlations and comparisons, a P value $<$ .05 was considered statistically significant to explore the possible relationship between neuropsychological scores and diffusion parameters.

RESULTS

Spatial Distribution of DTI/DKI Differences on Voxel-Based Analysis

Areas with decreased MK included the right frontal white matter, bilateral thalami, portions of the occipital white matter, corona radiata, corpus callosum, and portions of frontal and parietal white matter corresponding to the posterior segment of the superior longitudinal fasciculus (Fig 1). The decrease in FA was most extensive within the white matter (161,625 voxels), with its decrease amounting to 12,833 voxels (7.9%) (Fig 2). Significant MK, RK, and AK decreases were observed in 6180 voxels (3.8%), 3828 voxels (2.4%), and 3043 voxels (1.9%), respectively. In contrast, 9028 voxels (5.6%) showed a significant increase in MD; 10,062 (6.2%), in RD; and 548 (0.3%), in AD compared with controls. Figure 1 shows DKI/DTI overlap maps, with MK/RK/AK/FA decreases and MD/RD increases. Areas with FA decrease were more extensive than those with MK decrease; however, the posterior segment of the SLF showed a decrease in only MK/RK. The increase in MD/RD was remarkable in the corona radiata; however, the posterior segment of the SLF showed a decrease in MK/RK without an increase in MD/RD. Decreased AK was observed without changes in AD for the bilateral thalami, corona radiata, and portions of the temporo-occipital white matter. There was no cortical gray matter with altered DKI/DTI parameters in patients.

Correlation of DTI and DKI Parameters

Correlations between DKI and DTI parameters were examined in both the genu of the corpus callosum and the bilateral SLF (Table 2). In the corpus callosum of both controls and patients with MMD, MK correlated positively with FA ($r > 0.78$, $P < .01$), while inverse correlations with MK were found for MD/RD/AD ($r < -0.82$, $P < .001$). In the corpus callosum, RK correlated inversely with RD ($r < -0.84$, $P < .001$), and AK inversely correlated with AD of the corpus callosum ($r < -0.64$, $P < .001$). A significant correlation between MK and FA was observed in the left SLF of controls, but this was to a lesser degree compared with that in the corpus callosum. No correlation was found between MK and FA in the right SLF of controls. In both controls and patients, correlations between MK and MD/RD/AD were found in the right and left SLFs, albeit to a lesser degree than corpus callosum correlations. The results of correlation between DKI and DTI parameter values are summarized in Table 2.

Association of DKI/DTI Parameters with Neuropsychological Performance Tests

The DKI parameter (AK) showed significant correlations with motor intelligence quotient (IQ), full-scale IQ, perceptual organization, and processing speed evaluated on the Wechsler Adult Intelligence Scale-III (Fig 3A, $r > 0.42$, $P < .05$). Both DKI (MK) and DTI (FA, MD, and RD) parameters showed significant correlations with the TMT part B (Fig 3B, $r > 0.44$, $P < .05$). The Stroop test performance showed moderate positive correlations with MK, RK, and FA and negative correlations with MD, RD, and AD ($P < .05$). RST was associated with MK and AK ($P < .05$). The correlations between diffusion parameters and neuropsychological scores (Wisconsin Card Sorting Test, Stroop Test, CPT, and RST) are shown in Table 3.
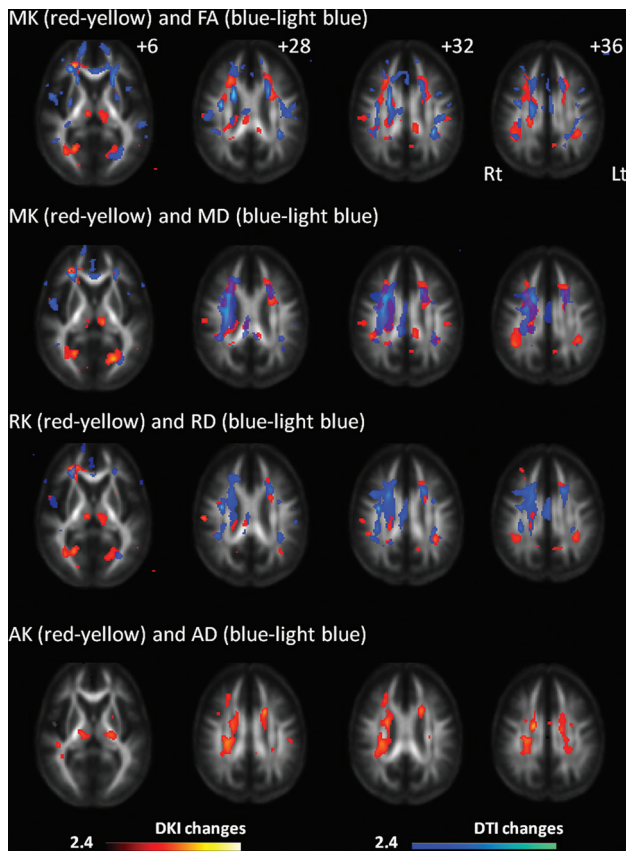
MK (red-yellow) and FA (blue-light blue)

MK (red-yellow) and MD (blue-light blue)

RK (red-yellow) and RD (blue-light blue)

AK (red-yellow) and AD (blue-light blue)

DKI changes   DTI changes

FIG 1. Changes in diffusional kurtosis imaging and diffusion tensor imaging parameters in Moyamoya disease shown in maps of 3 diffusional kurtosis parameters (mean kurtosis, radial kurtosis, and axial kurtosis) and 4 diffusion tensor parameters (fractional anisotropy, mean diffusivity, radial diffusivity, and axial diffusivity). Areas with significant changes in a combination of DKI/DTI parameters are as follows: decreased MK (red-yellow)/decreased FA (blue-light blue), decreased MK (red-yellow)/increased MD (blue-light blue), decreased RK (red-yellow)/increased RD (blue-light blue), and decreased AK (red-yellow)/increased and decreased AD (blue-light blue). Values from statistical parametric mapping analysis are projected onto axial sections of the average brain space of FA ($z = 12, 28, 32, 36$ mm). MK decrease is observed in the thalamus, a portion of the genu and body of the corpus callosum, corona radiata, frontoparietal subcortical white matter, and superior longitudinal fasciculus. RK decrease is observed in part of the frontoparietal subcortical white matter, thalamus, corona radiata, and occipital white matter. AK decrease is observed in the thalamus, temporo-occipital white matter, part of the SLF, and corona radiata. The radiologic convention is adopted, with the left side of the brain on the right side of axial panels. The color scale represents T values, with colored regions exceeding the significance threshold of $P < .01$ ($T = 2.42$) with a minimum cluster size of 50 voxels. Rt indicates right; Lt, left.

DISCUSSION

We explored the added benefit of diffusional kurtosis measurements in the assessment of ischemic burden due to chronic ischemia in adult MMD. This study confirmed our prior finding that chronic ischemia in MMD preferentially affects the microstructure of normal-appearing white matter.[3] Detecting microstructural changes due to chronic ischemia potentially enables early identification of patients at risk of cognitive impairment.[3,20] However, detecting microstructural changes has been hampered by the limited sensitivity of DTI in fiber-crossing areas.[7] In this study, DKI demonstrated microstructural changes, predominantly in the dorsal part of the deep white matter, where conventional MR imaging frequently demonstrates ischemic lesions.[21] The significant changes in DKI parameters were associated with neuropsychological scores reflecting general intelligence, executive function, attention, and working memory. Thus, DKI is considered a useful adjunct to conventional DTI, particularly for its ability to detect nascent microstructural changes in areas with abundant fiber crossings.

In this study, we demonstrated that DTI showed widespread regions with alterations in FA, MD, and RD. The finding is consistent with previous studies, in which DTI showed more extensive white matter changes compared with DKI parameters. Other studies have demonstrated superior sensitivity of DKI to detect white matter changes compared with DTI.[11,22,23] DKI showed significant decreases in frontoparietal subcortical structures and deep white matter. A decrease in DKI parameters, a shift of diffusional kurtosis toward free water diffusion, has commonly been interpreted as a reduction in tissue complexity.[24] Considering the location of the DKI alterations, a reduction in complexity is thought to reflect microstructural changes in myelin and/or axonal attenuation. In the corona radiata, DTI (MD/RD) demonstrated more significant changes compared with DKI (MK/RK). Deep white matter tracts are vulnerable to chronic ischemia because they are located in the terminal field of the blood supply. Myelin degeneration or increased periventricular extracellular fluid may increase RD, while tissue complexity in a radial direction may be maintained, in some part, by glial proliferation.[25] In a previous study, a trend toward decreased AD was found via analysis of tract-specific spatial statistics,[3] whereas the voxel-based analysis of the present study did not show definitive AD changes in white matter. AD decreases in axonal fragmentation; however, axonal degeneration or reduced axonal attenuation can increase AD. In contrast with AD, AK showed significant changes in the

Table 2: Correlation between DKI and DTI parameters[a]

	Corpus Callosum				Rt. SLF				Lt. SLF			
	CNT		MMD		CNT		MMD		CNT		MMD	
	r	P	r	P	r	P	r	P	r	P	r	P
MK vs FA	0.78	.000	0.80	.000	0.08	.715	0.60	.002	0.42	.047	0.47	.022
MK vs MD	−0.90	.000	−0.86	.000	−0.60	.002	−0.68	.000	−0.41	.049	−0.49	.017
MK vs RD	−0.90	.000	−0.87	.000	−0.54	.008	−0.73	.000	−0.49	.018	−0.55	.006
MK vs AD	−0.87	.000	−0.82	.000	−0.50	.014	−0.46	.028	−0.19	.386	−0.35	.101
RK and RD	−0.88	.000	−0.84	.000	−0.72	.000	−0.56	.005	−0.47	.025	−0.38	.072
AK and AD	−0.75	.000	−0.64	.000	−0.44	.036	−0.61	.001	−0.47	.025	−0.68	.000

Note:—Rt. indicates right; Lt., left; CNT, controls; *r*; Pearson product-moment correlation coefficient.
[a] All *P* values, except .715, .386, 101, and ,072, indicate significant correlation between DKI and DTI parameters.
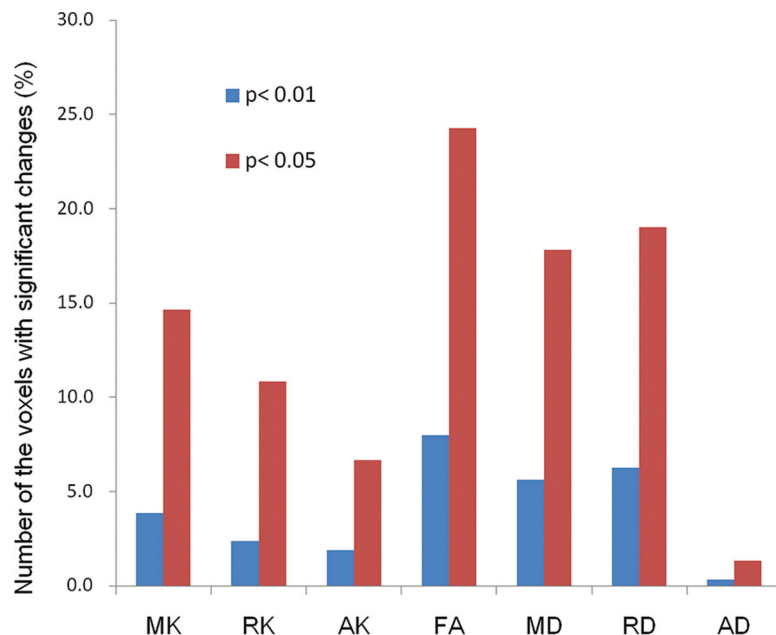
FIG 2. The bar graph indicates the number of the voxels with significant changes relative to the total number of white matter voxels in statistical parametric mapping comparing controls and patients with Moyamoya disease. Bar heights indicate decreases in MK/RK/AK/FA and increases in MD/RD/AD for 2 levels of threshold applied in group comparisons (blue, $P < .01$; red, $P < .05$, respectively).

corona radiata in the voxel-based analysis. Thus, alterations in AD would be marginal at best in patients, while tissue complexity parallel to the principal diffusion direction could be decreased in the corona radiata of patients. Weak correlations between FA and MK in the SLF of controls could be attributed to the crossing/ kissing of white matter fibers. The SLF contains abundant crossing fibers projecting from the corona radiata and corpus callosum.[18] Several fiber populations aligned along intersecting axes in 1 voxel would diminish anisotropy.[26]

The DKI parameters in patients showed moderate positive correlations with impaired general intelligence and frontal lobe dysfunction. These results are consistent with previous reports showing a relationship between cognitive performance and white matter fiber tracts integrating parietofrontal cortical areas.[27-29] In MMD, performance IQ is preferentially affected compared with verbal IQ.[1] In the present study, AK was significantly correlated with neuropsychological performance on tests evaluating executive function and working memory (motor IQ, perceptual organization, and processing speed), while no correlation was found with verbal IQ. In an experimental animal model of chronic white matter ischemia, damage to myelin preceded axonal damage, suggesting that the change in myelin is the primary pathologic event.[30] Our observation of a stronger correlation between AK, rather than AD, and general intellectual ability measured by the Wechsler Adult Intelligent Scale-III may imply that a reduction in axonal density and/or axonal degeneration, a more advanced stage of chronic ischemic injury, is better described by AK than AD. Previous investigations by using DTI and probabilistic tractography have shown correlations between neuropsychological examinations and the FA of subcortical white matter. Consistent with previous studies, we observed correlations between DTI parameters and the scores of neuropsychological tests evaluating

frontal lobe function in the present study. A significant correlation of FA/ MD/RD with scores on the Trail-Making Test suggests that demyelination alone could affect part of the frontal lobe functions.

Transient ischemic attack followed by hyperventilation is a characteristic symptom of childhood MMD, and syncope attacks are occasionally observed in both children and adults with MMD.[1] The spatial characteristics of nascent brain injury are important for understanding frontal-dominant neurocognitive dysfunction in adult MMD. Pyramidal neocortical neurons (layers 3, 5, and 6) in the prefrontal cortex are known to be highly vulnerable to hypoxic-ischemic insults.[31,32] These hypoxic-ischemic insults can damage the brain and potentially induce neuronal death or regression of dendritic structure.[8] We speculate that microstructural alteration precedes gross volumetric reductions in gray matter. Previous study has revealed gray matter atrophy in the posterior cingulate cortex, suggesting that more widespread gray matter changes might be observed in diffusion parameters, particularly in the frontal lobe.[3] DKI could reveal early microstructural changes less constrained by partial volume effects.[33] Nevertheless, despite discrete white matter damage, no substantial changes in diffusion parameters were found in the cortical gray matter in MMD. Pathologic tissue changes such as glial proliferation may underlie the lack of significant changes in the diffusion parameters of the cortices. A new diffusion MR imaging technique, including neurite orientation dispersion and density imaging, may detect subtle microstructural changes in the cortex and is potentially sensitive to initial ischemic changes before the overt volumetric reductions.[34,35]

The present study revealed microstructural change in the thalamus, a finding that has never been emphasized with regard to cognitive function in MMD. The mediodorsal thalamus connects to the prefrontal cortex. This is potentially important because innervation of the thalamoprefrontal circuit could modulate prefrontal neural circuits, which are associated with cognitive as well as affective performance.[36]

There are several limitations to this study. The statistical power to detect group differences in DKI parameters is significantly influenced by the number of subjects in a study.[37] Therefore, the spatial characteristics of the DKI/DTI alterations found in this study may not represent the topography of ischemic burden in adult MMD.[37] We extracted DKI/DTI values from the contrast T maps generated from group comparisons between controls and patients to explore the relationship between abnormal diffusion parameters in patients and neuropsychological test performance. Although we found an association with neuropsychological test scores, voxel-based correlation analysis would per-
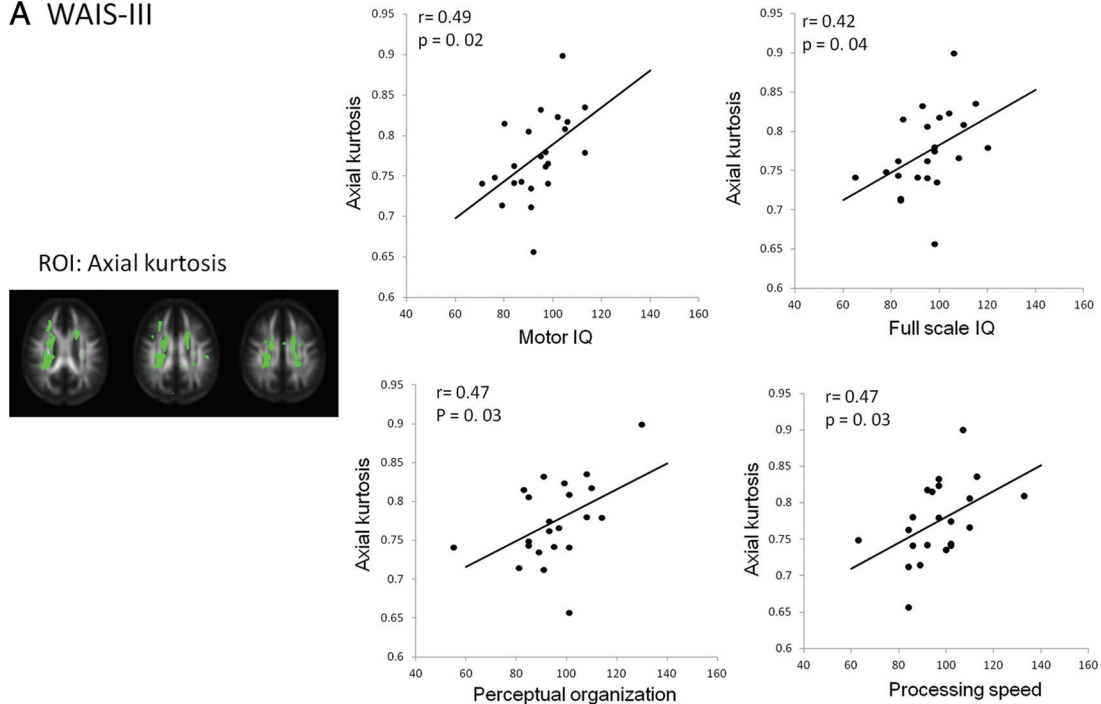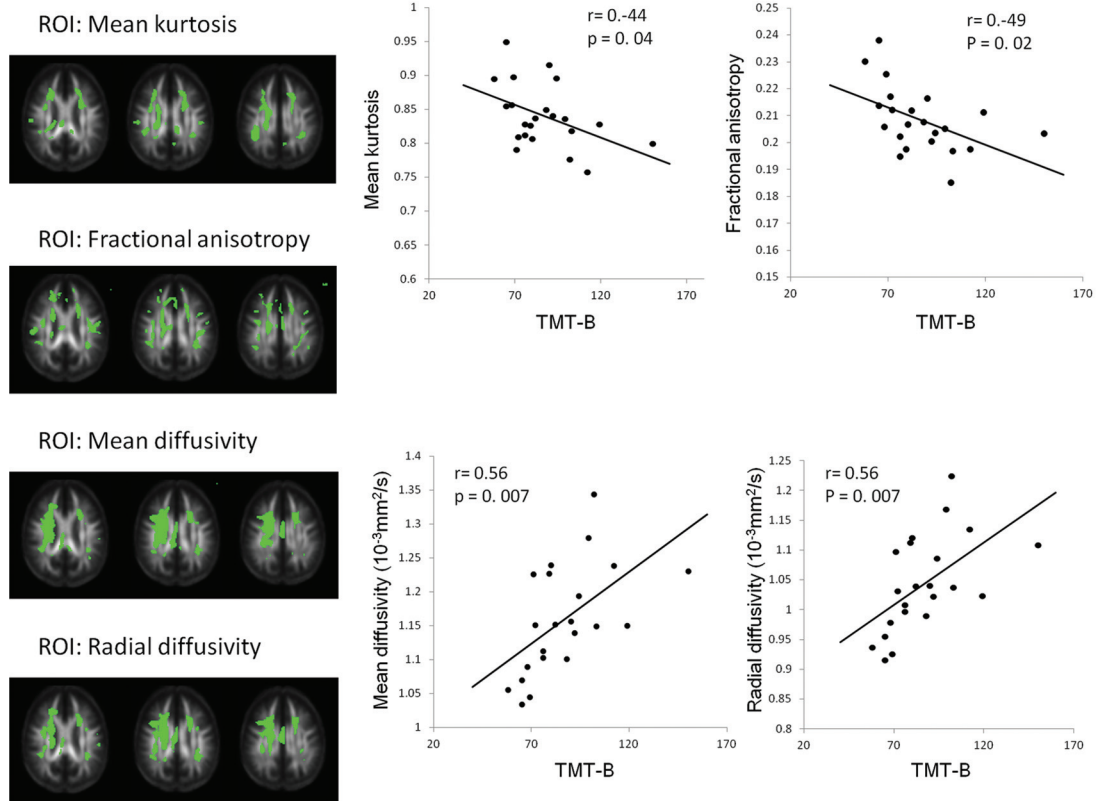
FIG 3. Scatterplots indicating a significant correlation between neuropsychological test performance and diffusion parameters. Pearson moment-production correlation coefficient r and P values are demonstrated in each scatterplot. ROIs (green) for each parameter (AK, MK, FA, MD, and RD) are demonstrated with FA template images generated from 23 controls and 23 patients. *A*, Performance scores evaluated on the Wechsler Adult Intelligent Scale-III are significantly associated with axial kurtosis. Axial kurtosis is positively correlated with full-scale IQ ($r = 0.42$, $P = .04$) and subscores such as motor IQ ($r = 0.49$, $P = .02$), perceptual organization ($r = 0.47$, $P = .03$), and processing speed ($r = 0.47$, $P = .03$). *B*, Trail-Making Test, part B is inversely correlated with DKI/DTI parameters (MK; $r = -0.44$, $P = .04$; and FA; $r = -0.49$, $P = .02$) and positively correlated with DTI parameters (MD; $r = 0.56$, $P = .007$; and RD; $r = 0.56$, $P = .007$).

Table 3: Correlations of diffusion parameters with neuropsychological examinations[a]

	WCST	Stroop	CPT	RST
MK	–	.004[b]	–	.048[b]
RK	–	.007[b]	–	–
AK	–	.045[c]	–	.036[c]
FA	–	.024[b]	–	–
MD	–	.012[b]	–	–
RD	–	.014[b]	–	–
AD	–	.031[c]	–	–

Note:—WCST indicates Wisconsin Card Sorting Test, Stroop; Stroop test.
[a] Data are *P* values. Correlations of diffusional kurtosis imaging and diffusion tensor imaging parameters with neuropsychological examinations were evaluated in patients with MMD. Three diffusional kurtosis parameters (MK, RK, and AK) and 4 diffusion tensor parameters (FA, MD, RD, and AD) were analyzed. Diffusion parameters and locations that demonstrated significant relationships with clinical variables follow.
[b] Two-tailed *t* test.
[c] One-tailed *t* test.

mit an objective evaluation of the neural substrates associated with cognitive impairment. Finally, we used a combination of b-values of 0 and 1000 s/mm^2 for DTI. DTI parameters are reported as dependent on b-values. For DKI, the b-values of 0, 1000, and 2000 s/mm^2 used in the present study would be feasible for practical clinical applications. Nevertheless, a different combination of b-values and methods for parameter estimation could alter the relationship between DKI and DTI with regard to sensitivity and specificity, which requires further investigation.[21]

CONCLUSIONS

The results of the present study suggest an additional value of DKI as an adjunct to DTI. DKI parameters can become useful neuroimaging markers to track ischemic burden in adult MMD.

REFERENCES

1. Kuroda S, Houkin K. **Moyamoya disease: current concepts and future perspectives.** *Lancet Neurol* 2008;7:1056–66 CrossRef Medline
2. Karzmark P, Zeifert PD, Bell-Stephens TE, et al. **Neurocognitive impairment in adults with Moyamoya disease without stroke.** *Neurosurgery* 2012;70:634–38 CrossRef Medline
3. Kazumata K, Tha KK, Narita H, et al. **Chronic ischemia alters brain microstructural integrity and cognitive performance in adult Moyamoya disease.** *Stroke* 2015;46:354–60 CrossRef Medline
4. Tha KK, Terae S, Nakagawa S, et al. **Impaired integrity of the brain parenchyma in non-geriatric patients with major depressive disorder revealed by diffusion tensor imaging.** *Psychiatry Res* 2013;212:208–15 CrossRef Medline
5. Basser PJ, Mattiello J, LeBihan D. **MR diffusion tensor spectroscopy and imaging.** *Biophys J* 1994;66:259–67 Medline
6. Jensen JH, Helpern JA, Ramani A, et al. **Diffusional kurtosis imaging: the quantification of non-gaussian water diffusion by means of magnetic resonance imaging.** *Magnetic Reson Med* 2005;53:1432–40 Medline
7. Back SA. **Cerebral white and gray matter injury in newborns: new insights into pathophysiology and management.** *Clin Perinatal* 2014;41:1–24 CrossRef Medline
8. Zhang S, Boyd J, Delaney K, et al. **Rapid reversible changes in dendritic spine structure in vivo gated by the degree of ischemia.** *J Neurosci* 2005;25:5333–38 Medline
9. Fieremans E, Jensen JH, Helpern JA. **White matter characterization with diffusional kurtosis imaging.** *Neuroimage* 2011;58:177–88 CrossRef Medline
10. Li X, Gao J, Hou X, et al. **Diffusion kurtosis imaging with tract-based spatial statistics reveals white matter alterations in preschool children.** *Conf Proc IEEE Eng Med Biol Soc* 2012;2012:2298–301 CrossRef Medline
11. Coutu JP, Chen JJ, Rosas HD, et al. **Non-Gaussian water diffusion in aging white matter.** *Neurobiol Aging* 2014;35:1412–21 CrossRef Medline
12. Gong NJ, Wong CS, Chan CC, et al. **Aging in deep gray matter and white matter revealed by diffusional kurtosis imaging.** *Neurobiol Aging* 2014;35:2203–16 CrossRef Medline
13. Caverzasi E, Henry RG, Vitali P, et al. **Application of quantitative DTI metrics in sporadic CJD.** *Neuroimage Clin* 2014;4:426–35 CrossRef Medline
14. Weber RA, Hui ES, Jensen JH, et al. **Diffusional kurtosis and diffusion tensor imaging reveal different time-sensitive stroke-induced microstructural changes.** *Stroke* 2015;46:545–50 CrossRef Medline
15. Grinberg F, Farrher E, Ciobanu L, et al. **Non-Gaussian diffusion imaging for enhanced contrast of brain tissue affected by ischemic stroke.** *PLoS One* 2014;9:e89225 CrossRef Medline
16. Umesh Rudrapatna S, Wieloch T, Beirup K, et al. **Can diffusion kurtosis imaging improve the sensitivity and specificity of detecting microstructural alterations in brain tissue chronically after experimental stroke? Comparisons with diffusion tensor imaging and histology.** *Neuroimage* 2014;97:363–73 CrossRef Medline
17. Tabesh A, Jensen JH, Ardekani BA, et al. **Estimation of tensors and tensor-derived measures in diffusional kurtosis imaging.** *Magn Reson Med* 2011;65:823–36 CrossRef Medline
18. Reijmer YD, Leemans A, Heringa SM, et al; Vascular Cognitive Impairment Study group. **Improved sensitivity to cerebral white matter abnormalities in Alzheimer's disease with spherical deconvolution based tractography.** *PLoS One* 2012;7:e44074 CrossRef Medline
19. Wakana S, Jiang H, Nagae-Poetscher LM, et al. **Fiber tract-based atlas of human white matter anatomy.** *Radiology* 2004;230:77–87 Medline
20. Cheng HL, Lin CJ, Soong BW, et al. **Impairments in cognitive function and brain connectivity in severe asymptomatic carotid stenosis.** *Stroke* 2012;43:2567–73 Medline
21. Schmidt R, Seiler S, Loitfelder M. **Longitudinal change of small-vessel disease-related brain abnormalities.** *J Cereb Blood Flow Metab* 2015 Apr 22. [Epub ahead of print] CrossRef Medline
22. Kamagata K, Tomiyama H, Hatano T, et al. **A preliminary diffusional kurtosis imaging study of Parkinson disease: comparison with conventional diffusion tensor imaging.** *Neuroradiology* 2014;56:251–58 CrossRef Medline
23. Fieremans E, Benitez A, Jensen JH, et al. **Novel white matter tract integrity metrics sensitive to Alzheimer disease progression.** *AJNR Am J Neuroradiol* 2013;34:2105–12 CrossRef Medline
24. Steven AJ, Zhuo J, Melhem ER. **Diffusion kurtosis imaging: an emerging technique for evaluating the microstructural environment of the brain.** *AJR Am J Roentgenol* 2014;202:W26–33 CrossRef Medline
25. Cechetti F, Pagnussat AS, Worm PV, et al. **Chronic brain hypoperfusion causes early glial activation and neuronal death, and subsequent long-term memory impairment.** *Brain Res Bull* 2012;87:109–16 CrossRef Medline

26. Jbabdi S, Behrens TE, Smith SM. **Crossing fibres in tract-based spatial statistics.** *Neuroimage* 2010;49:249–56 CrossRef Medline

27. Gläscher J, Rudrauf D, Colom R, et al. **Distributed neural system for general intelligence revealed by lesion mapping.** *Proc Natl Acad Sci U S A* 2010;107:4705–09 CrossRef Medline

28. Deary IJ, Weiss A, Batty GD. **Intelligence and personality as predictors of illness and death: how researchers in differential psychology and chronic disease epidemiology are collaborating to understand and address health inequalities.** *Psychol Sci Public Interest* 2010;11: 53–79 CrossRef Medline

29. Barbey AK, Colom R, Solomon J, et al. **An integrative architecture for general intelligence and executive function revealed by lesion mapping.** *Brain* 2012;135:1154–64 CrossRef Medline

30. Kurumatani T, Kudo T, Ikura Y, et al. **White matter changes in the gerbil brain under chronic cerebral hypoperfusion.** *Stroke* 1998;29: 1058–62 Medline

31. Lin CS, Polsky K, Nadler JV, et al. **Selective neocortical and thalamic cell death in the gerbil after transient ischemia.** *Neuroscience* 1990; 35:289–99 Medline

32. Fukuda A, Muramatsu K, Okabe A, et al. **NMDA receptor-mediated differential laminar susceptibility to the intracellular Ca2+ accu-mulation induced by oxygen-glucose deprivation in rat neocortical slices.** *J Neurophysiol* 1998;79:430–38 Medline

33. Yang AW, Jensen JH, Hu CC, et al. **Effect of cerebral spinal fluid suppression for diffusional kurtosis imaging.** *J Magn Reson Imaging* 2013;37:365–71 CrossRef Medline

34. Jelescu IO, Veraart J, Adisetiyo V, et al. **One diffusion acquisition and different white matter models: how does microstructure change in human early development based on WMTI and NODDI?** *Neuroimage* 2015;107:242–56 CrossRef Medline

35. Zhang H, Schneider T, Wheeler-Kingshott CA, et al. **NODDI: practical in vivo neurite orientation dispersion and density imaging of the human brain.** *Neuroimage* 2012;61:1000–16 CrossRef Medline

36. Ferguson BR, Gao WJ. **Development of thalamocortical connections between the mediodorsal thalamus and the prefrontal cortex and its implication in cognition.** *Front Hum Neurosci* 2014;8:1027 Medline

37. Szczepankiewicz F, Lätt J, Wirestam R, et al. **Variability in diffusion kurtosis imaging: impact on study design, statistical power and interpretation.** *Neuroimage* 2013;76:145–54 CrossRef Medline